INPE – National Institute for Space Research
São José dos Campos – SP – Brazil – May 16-20, 2016

SYNCHRONIZATION DETECTION AND CHARACTERIZATION THROUGH MIXED STATE EMBEDDING AND RECURRENCE QUANTIFICATION ANALYSIS

Leonardo L. Portes[1] *and Luis A. Aguirre*[2]

[1]Dep. de Engenharia Eletrônica/UFMG, Belo Horizonte, Brasil, ll.portes@gmail.com
[2]Dep. de Engenharia Eletrônica/UFMG, Belo Horizonte, Brasil, aguirre@ufmg.br

Abstract: We address the detection and characterization of synchronization in coupled nonlinear oscillators by comparing the temporal and magnitude signatures unfolded in both *mixed state* and *single state spaces* of each subsystem. Such properties, as the complexity estimated by the Shannon entropy, are quantified by recurrence quantification analysis (RQA) and by using a Poincaré section to separate the temporal and amplitude signatures of the signals.

keywords: Synchronization in Nonlinear Systems, Time Series Analysis, Analysis and Control of Nonlinear Dynamical Systems with Practical Applications, Recurrence Quantification Analysis, Shannon Entropy.

1. INTRODUCTION

The study of synchronization phenomena of chaotic systems in networks has evolved rapidly, with a growing interest in the areas of patterns formation and clustering synchronization [1]. Several types of synchronous regimes were reported so far, ranging from phase synchronization (PS), lag synchronization (LS), generalized synchronization (GS) and complete synchronization [2] (to mention just a few). Intermittent versions of some of those regimes were found near transitions (*e.g.*, for characterization of eyelet and ring intermittency, see [3] and references therein). PS is characterized by the correlation of the time scales, while the amplitudes remain low correlated and chaotic [4]. In CS, both the time scales and the amplitudes are correlated, hence the states of the coupled subsystems are equal: $\vec{x}_1 = \vec{x}_2$.

A known problem in the study of chaotic phase synchronization is that there is no general and straightforward way to estimate the phases $\phi_j(t)$ and amplitudes $A_j(t)$ of a given system j [2]. For more complex funnel like dynamics, a phase estimate is obtained case by case.

Here we investigate the use of time series extracted from the peak-to-peak signals (equivalent to a Poincaré section), as a possible general way to characterize synchronization: by disentangling the *time* and amplitude information provided by the measurement of the flow. Given a time series x, we consider as the work data the time series of the (i) magnitude of the peaks and the (ii) inter-peak time interval (also called return times). We investigate if type (ii) time series captures the information about the phase coupling, while the type (ii) retrieves information about the coupling of the amplitudes.

Recently, we provided numerical evidence that the recurrence quantification analysis (RQA) variables are estimated more accurately from a Poincaré section of a flow, than from the flow data itself [5] (as already reported for the Shannon entropy, investigated in [6]). In the present work, we apply the RQA with the work data using two different approaches: single and mixed state embeddings.

2. PURPOSE

Specifically, two questions are addressed. First, to what extend, if any, can the analysis of types (i) and (ii) time series detect and characterize the time and amplitude properties of different synchronized regimes? Second, does the use of both mixed state and single state spaces provide more information about the synchronization behavior?

3. METHODS

We consider two bidirectionaly coupled Rössler oscillators

$$\begin{aligned}\dot{x}_{1,2} &= -\omega_{1,2}y_{1,2} - z_{1,2},\\ \dot{y}_{1,2} &= \omega_{1,2}x_{1,2} + ay_j + c(y_{2,1} - y_{1,2}),\\ \dot{z}_{1,2} &= 0.1 + z_{1,2}(x_{1,2} - 8.5)\end{aligned} \tag{1}$$

with individual natural frequencies $\omega_{1,2} = (1, 1.02)$ and with natural chaotic phase-coherent regime ($a = 0.15$). Equation (1) was integrated (time steps of 0.01 s) for each value of the coupling strength $c \in [0.001, 0.2]$ and the initial transient was removed. The time series $y^{(1)}(t)$ and $y^{(2)}(t)$ (systems 1 and 2, respectively) were resampled ($T_s = 0.07$ s) and the final length was $N = 142858$ data points (total time of 10^4 s). The peaks of each $y^{(j)}(t)$ ($j = 1, 2$) were detected, providing the time series of their magnitude, $\{y_i^{(j)}\}$, and the inter-peak interval, $\{\tau_i^{(j)}\}$.

RQA was performed on the work data $y^{(j)}$ and $\tau^{(j)}$ using the time delay embedding with two approaches. In the first one, each time series were embedded into their own m-dimensional space $\mathbf{R}^m$, yielding the vectors $\vec{y}_i^{(j)} = (y_i^{(j)}, y_{i+l}^{(j)}, ..., y_{i+(m-1)l}^{(j)})$ and $\vec{\tau}_i^{(j)} = (\tau_i^{(j)}, \tau_{i+l}^{(j)}, ..., \tau_{i+(m-1)l}^{(j)})$. In the second approach, the mixed state embeddings $\vec{y}_i^{(1,2)} = (y_i^{(1)}, y_{i+l}^{(1)}, ..., y_{i+(m-1)l}^{(1)}; y_i^{(2)}, y_{i+l}^{(2)}, ..., y_{i+(m-1)l}^{(2)})$ and $\vec{\tau}_i^{(1,2)} = (\tau_i^{(1)}, \tau_{i+l}^{(1)}, ..., \tau_{i+(m-1)l}^{(1)}; \tau_i^{(2)}, \tau_{i+l}^{(2)}, ..., \tau_{i+(m-1)l}^{(2)})$ were used. Here, we call them the single state space (s-ss) and mixed state space (m-ss) approaches, respectively.

In both cases, $m = 4$ and the delay $l = 1$ data point. The RQA threshold ϵ corresponded to 10% of the maximum distance in the reconstructed phase space. The following RQA variables were used: recurrence rate ($\%REC$), "determinism" ($\%DET$), divergence (DIV) and shannon entropy (S) as defined in [6]. For the sake of clarity, the following notation is used for a given RQA variable, as exemplified by the entropy S: $S_\gamma^{(j^*)}$, where $\gamma = (PP, IPI)$ is the type of work data used and j^* refers to system 1, 2, with the s-ss, or is $1, 2$ when the m-ss is considered. From those variables, we compute the ratio DET/RR and estimate the mutual information from $I_{PP} = S_{PP}^{(1)} + S_{PP}^{(2)} - S_{PP}^{(1,2)}$ and $I_{IPI} = S_{IPI}^{(1)} + S_{IPI}^{(2)} - S_{IPI}^{(1,2)}$.

In order to gain insight into the synchronization behavior with increasing coupling c, we conducted two complementary analysis. First, the single-variable multivariate singular spectrum analysis (SM-SSA) [7–9] was applyied with the variable y_j of each system. Second, a straightforward analysis of the phase difference $\Delta\phi(t) = |\phi(t)_1 - \phi(t)_2|$ [2] was conducted. For each system, the phase was estimated by $\phi(t)_j = \mathrm{arctg}(y_j/x_j)$ [10]. PS is characterized by a bounded phase difference $\Delta\phi(t) = |m\phi(t)_1 - n\phi(t)_2| \leq \mathrm{const}$, and low correlation of the amplitudes. Finally, in order to quantify the "quality" of synchronization, we compute the *degree of synchronization* as characterized by $\langle s_j \rangle$ [10, p. 158], where $s_j = \sin^2\left(\frac{\phi_2(\mathrm{t}) - \phi_1(\mathrm{t})}{2}\right)$ characterizes the instantaneous phase difference between systems $j = 1$ and $j = 2$, and $\langle \cdot \rangle$ is the time average. The average $\langle s_j \rangle$ is 0.5 for uncorrelated phases.

4. RESULTS

The characterization of synchronization along an increasing c is performed in Sec. 4.1. The RQA with the PP and IPI series, in both s-ss and m-ss approaches, is presented in Sec. 4.2.

4.1. Preliminary analysis

We first present the results of the SM-SSA, which give a general overview of the synchronization behavior. Figure 1 shows the singular spectrum λ^* [*modified* variances, panel (a)] and the participation index difference between the oscillatory mode k of the systems, $\Delta\pi_k = \sum \pi_{1,k} - \sum \pi_{2,k}$ [panel (b)]. Both *suggests* the onset of PS near $c \approx 0.02$. Surprisingly, this technique captured what seems to be a second transition near $c \approx 0.08$, which is more visible with $\Delta\pi_Y$. So, we consider three ranges regarding synchronization and two transitions. Accordingly, six values (dashed vertical lines) of the coupling strength were chosen to guide the following discussion and to perform a straightforward phase analysis: $\{c_1, c_2, c_3, c_4, c_5, c_6\} \approx \{0.0013, 0.016, 0.024, 0.060, 0.1, 0.2\}$.

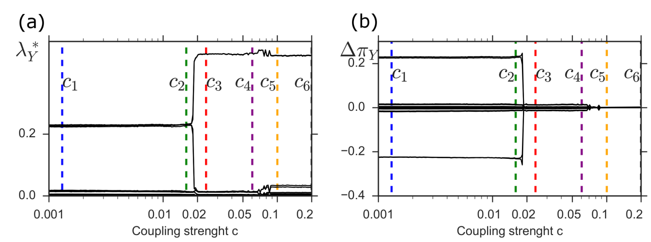

Figure 1 – SM-SSA analysis of two coupled Rössler systems, with increasing coupling c. (a) modified variances, (b) difference between the participation index of the oscillators.

The phase difference $\Delta\phi(t)$, Fig. 2.(a), is unbounded for $c = \{c_1, c_2\}$, implying that these regimes are not synchronous. For $c = c_3$ to c_6, the phases are completely locked. Hence, the phases are synchronized, while the amplitudes [Fig. 2.(b)] become increasingly more correlated. At c_3, the low correlation of amplitudes suggests PS. At $c = c_4$, they are more correlated but no structure is seen. At $c = c_5, c_6$, if one *zooms in* in the two last plots (not shown), the image of a time-delay embedded Rössler system with a small value of the delay is seen. This feature is a signature of LS. These results corroborates the information given by the SM-SSA analysis, for which at least phase synchronization is present for $c > 0.02$, and allows to corroborate the existence and characterize the second transition at $c \approx c_5$ as the onset of LS. Finally, Fig. 2.(c) indicates that the phase-coherent topology of each system is preserved, which guarantees the

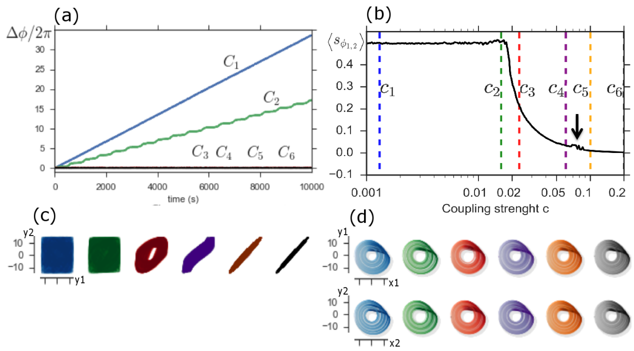

Figure 2 – Phase and amplitude analysis of the coupled systems. (a) Instantaneous phase difference $\Delta\phi(t)$. (b) Degree of synchronization $\langle s_j \rangle$ with an increasing c. (c) Plots of $y_1(t)$ *vs.* $y_2(t)$. (d) Projections of the trajectories of systems $j = 1, 2$ onto the xy plane (z is represented by the shading).

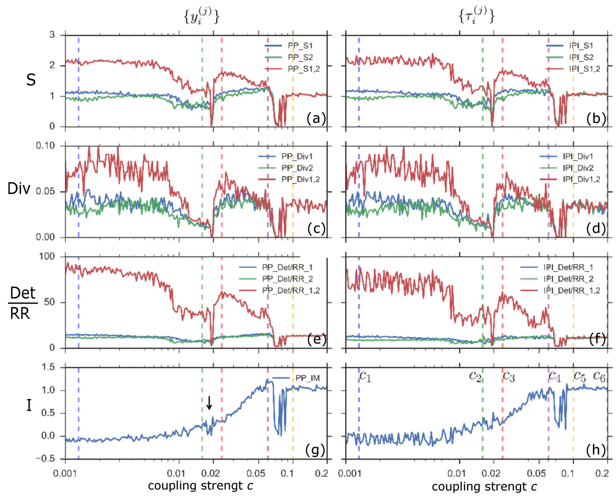

Figure 3 – RQA performed with the time series $\{y_i^{(j)}\}$ and $\{\tau_i^{(j)}\}$ with the single and mixed state embedding approaches.

appropriateness of the phase estimative applied here.

It is pertinent to access "continuously" the synchronization along the increasing c. For this, Fig. 2(b) shows the degree of synchronization $\langle s_j \rangle$. It agrees with the sliced analysis, showing the onset of a "high-quality" synchronism after $c \approx 0.02$. Interesting, this analysis shows a deviation from the general increasing of quality for $c_4 < c < c_5$ (the second transition suggested by SV-SSA), and is signed by a black arrow. Taken together, the results suggest that one has three distinct ranges regarding synchronization: (I) no-synchronization for $c < c_2$, (II) *at least* PS at $c_3 < c < c4$, and (III) LS with decreasing lag for $c > c_5$. This is a clearly trend in the direction to CS. At a more general level of analysis, one could consider only two ranges: no-synchronization and *at least* PS (joining ranges II and III), with a critical coupling strength $c_c \approx 0.02$.

4.2. RQA with the single state embedding and mixed state embedding approaches

Figure 3 shows the results of the RQA with the $\{y_i^{(j)}\}$ and $\{\tau_i^{(j)}\}$ time series (left and right panels, respectively). The six dashed vertical lines are the same used in the previous section to indicate the selected coupling strengths that guide the discussion. For the sake of space, only S, DIV, Det/RR and I are shown. The general features observed a similar with $\%RR$ and $\%DET$.

The following features are visible. First, the behavior of the variables computed from the $\{y_i^{(j)}\}$ and $\{\tau_i^{(j)}\}$ time series is similar, except the plateau near c_4 observed in I_τ [Fig. 3(h)]. Hence, in the following our discussion of the RQA results are equivalent to both approaches. Second, the transition ranges $c_2 - c_3$ and $c_4 - c_5$ are clearly discernible by the high spikes of $\%RR$ and $\%DET$ (not shown), and the valleys with S [Fig. 3(a,b)] and DIV [Fig. 3(c,d)], for both single and mixed state embedding approaches). With DET/RR [Fig. 3(e,f)], the valley indicating the first transition $c_2 - c_3$ is present only for the mixed state embedding. Third, all RQA variables show a change in the initial horizontal trend, preceding the spike/valley of transition $c_2 - c_3$, which is much more visible in the mixed state embedding with the variables $\%Det$, S, DIV and Det/RR. Fourth, a plateau is found after the second transition $c > c_5$, for which a given RQA variable has the same value for both single and mixed state embeddings, suggesting that the systems are identical. Finally, the estimate of the mutual information, Fig. 3(g,h), is the only that presents a (small) difference between the $\{y_i^{(j)}\}$ and $\{\tau_i^{(j)}\}$ time series. A plateau preceding c_4 is seen in I_τ but not in I_y, which can be further investigated. I_y fluctuates less than I_τ, and is the only to show a signal of the transition region $c_2 - c_3$ (signed with a black arrow). The second transition, $c_4 - c_5$, is visible as a deep valley in both approaches.

5. DISCUSSION

One of the main goals of the present work was to verify the possibility to access the coupling of time scales (implying PS) and the amplitudes (implying LS or CS) in a untangled way, through the use of the peak-to-peak signals $\{y_i^{(j)}\}$ and $\{\tau_i^{(j)}\}$. However, the results obtained with both time series were identical, with the exception of a small plateau in the mutual information I_τ before the second transition, $c < c_4$, and is currently being investigated.

The identical results obtained with $\{y_i^{(j)}\}$ and $\{\tau_i^{(j)}\}$ could be analysed and more deeply understood with the *peak-to-peak dynamics* unified approach proposed in [11], which allows the quantification of the entrainment between their dynamics. Our results could be associated to the existence of a functional relationship $y_i = Y^T(\tau_i)$. This approach provides more tools and concepts to explore our hypothesis, and future studies will be conducted.

All RQA variables detected the LS regime. It was characterized by the identical values of the RQA variables with the mixed state embedding compared with the single state embeddings. Strictly speaking, the systems are not identical at the same time, but one is the lagged copy of the other.

The RQA was not able to precisely detect the more subtle PS regime, but it showed an increasing similarity between the values obtained with the mixed state embedding and those with single state embedding. *E.g.*, DIV with the mixed state embedding (mse) begins a trending towards the values with single state embeddings (sse) at $c \approx 0.007$ and became very close (but not identical) at $c \approx 0.011$. After the first transition (near $c = c_3$), that difference increases, but Div_{mse} stays at a lower value than the observed at the non-synchronous regime (the opposite occurs for the values of Div_{sse}, which are observed at higher values than before). These values of DIV start to approximate again and became identical near and after the second transition (at $c > c_4$). This general behavior could lead to an appropriate index to characterize the onset of PS and LS and are being currently investigated, with no necessity of an *a priori* phase for frequency estimative.

Another feature is the early sign of PS (modification of the initial trend of the RQA variables) given by the mixed state embedding approach. The real nature of the systems dynamics at these coupling values and their fingerprint in the RQA will be taken into account in future research.

6. CONCLUSIONS

It was not possible to untangle the synchronization features of the phases (time scales) and amplitudes with the peak-to-peak approach as analysed with the RQA, namelly by comparing the results of the time series $\{y_i^{(j)}\}$ and $\{\tau_i^{(j)}\}$ with single and mixed state embedding approaches. Currently, we are exploring the tools and concepts of the *peak-to-peak dynamics* unified approach [11] to deepen the investigation of our main hypotheses.

The use of the mixed state embedding, in addition to the single one, provided some hints of profound modifications of the systems dynamics observed along the increasing values of the coupling strength. This could lead in a appropriate index to characterize synchronization regimes. Since there is no general way to access the phases of a given system, an index independent of a phase definition would be a welcome feature.

Another topic is the possibility to retrieve the information of the synchronization process observing only one system, and not both. As seen in the single state embedding approach, enhanced by the with of the Poincarè section, the RQA features changed along the increasing of the coupling strength, suggesting the possibility of measuring just one system $j = 1$ or $j = 2$. To what extend one could clearly associate these changes to the different synchronization regimes remains for future research.

ACKNOWLEDGMENTS

This work was carried out with CNPq support, Conselho Nacional de Desenvolvimento Científico e Tecnológico - Brazil.

References

[1] A. Pikovsky and M. Rosenblum, "Dynamics of globally coupled oscillators: Progress and perspectives," *Chaos: An Interdisciplinary Journal of Nonlinear Science*, vol. 25, p. 097616, Sept. 2015.

[2] S. Boccaletti, J. Kurths, G. Osipov, D. Valladares, and C. Zhou, "The synchronization of chaotic systems," *Physics Reports*, vol. 366, pp. 1–101, 2002.

[3] O. I. Moskalenko, A. A. Koronovskii, A. E. Hramov, M. O. Zhuravlev, and Y. I. Levin, "Cooperation of deterministic and stochastic mechanisms resulting in the intermittent behavior," *Chaos, Solitons & Fractals*, vol. 68, pp. 58–64, nov 2014.

[4] M. G. Rosenblum, a. S. Pikovsky, and J. Kurths, "Phase synchronization of chaotic oscillators," *Physical Review Letters*, vol. 76, no. 11, pp. 1804–1807, 1996.

[5] L. L. Portes, R. N. Benda, H. Ugrinowitsch, and L. A. Aguirre, "Impact of the recorded variable on recurrence quantification analysis of flows," *Physics Letters A*, vol. 378, pp. 2382–2388, jun 2014.

[6] C. Letellier, "Estimating the Shannon Entropy: Recurrence Plots versus Symbolic Dynamics," *Physical Review Letters*, vol. 96, p. 254102, jun 2006.

[7] L. L. Portes and L. A. Aguirre, "Matrix formulation and singular-value decomposition algorithm for structured varimax rotation in multivariate singular spectrum analysis," *Physical Review E*, vol. 93, p. 052216, may 2016.

[8] L. L. Portes and L. A. Aguirre, "Observability analysis suggests a single-variable approach for the multivariate singular spectrum analysis in the study of phase synchronization," *Manuscript submitted for publication*.

[9] A. Groth and M. Ghil, "Multivariate singular spectrum analysis and the road to phase synchronization," *Physical Review E - Statistical, Nonlinear, and Soft Matter Physics*, vol. 84, no. 3, pp. 1–12, 2011.

[10] G. V. Osipov, J. Kurths, and C. Zhou, *Synchronization in Oscillatory Networks*. Springer Series in Synergetics, Berlin, Heidelberg: Springer Berlin Heidelberg, 1st ed., 2007.

[11] M. Candaten and S. Rinaldi, "Peak-to-peak dynamics: a critical survey," *International Journal of Bifurcation and Chaos*, vol. 10, pp. 1805–1819, aug 2000.